



Design of an Ion Source for 3He Fusion in a Low Pressure IEC Device

G.R. Piefer, J.F. Santarius, R.P. Ashley, G.L. Kulcinski

September 2004

UWFDM-1255

Presented at the 16th ANS Topical Meeting on Fusion Energy, 14–16 September 2004, Madison WI.

FUSION TECHNOLOGY INSTITUTE

UNIVERSITY OF WISCONSIN

MADISON WISCONSIN

**Design of an Ion Source for 3He Fusion in a
Low Pressure IEC Device**

G.R. Piefer, J.F. Santarius, R.P. Ashley, G.L.
Kulcinski

Fusion Technology Institute
University of Wisconsin
1500 Engineering Drive
Madison, WI 53706

<http://fti.neep.wisc.edu>

September 2004

UWFDM-1255

Presented at the 16th ANS Topical Meeting on Fusion Energy, 14–16 September 2004, Madison WI.

DESIGN OF AN ION SOURCE FOR ^3He FUSION IN A LOW PRESSURE IEC DEVICE

Gregory R. Piefer, John F. Santarius, Robert P. Ashley, Gerald L. Kulcinski

Fusion Technology Institute—University of Wisconsin Madison: 1500 Engineering Drive, Madison, WI, USA, 53706, grpiefer@wisc.edu

Recent developments in helicon ion sources and Inertial Electrostatic Confinement (IEC) device performance at UW-Madison have enabled low pressure ($< 50 \mu\text{torr}$, 6.7 mPa) operating conditions that should allow the ^3He - ^3He fusion reaction to be observed in an IEC device. An ion source capable of delivering a $\sim 10 \text{ mA}$ ^3He ion beam into an IEC device with minimal neutral gas flow has been designed and tested. Furthermore, a new IEC device that has never been operated with deuterium has been constructed to avoid D - ^3He protons from obstructing the ^3He - ^3He reaction product spectrum, and to minimize Penning ionization of deuterium by excited helium, which in the past is suspected to have limited the ionized density of He. These developments make it possible to study beam-background ^3He - ^3He fusion reactions with $> 300 \text{ mA}$ recirculating ion currents.

I. INTRODUCTION

I.A. IEC Basics

Inertial Electrostatic Confinement (IEC) fusion devices as they exist today were first built and studied by Philo. T. Farnsworth¹ and one of his associates, Robert L. Hirsch.² Since then, most IEC experiments have operated in a simple configuration, consisting of either two concentric spherical or coaxial cylindrical grids. A large negative potential difference is created between the grids causing a radial electric field, which attracts positively charged ions. In the most basic model these ions oscillate through the core until they collide and fuse or are lost to a collision with the grid. Since the ions are directed almost purely radially, they converge to a small core as they pass through the cathode, creating a high ion density, as depicted in Fig. 1.

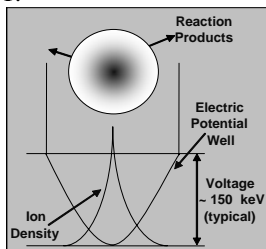


Figure 1: Basic IEC theory

The advantage of this system over other confinement techniques is that it is possible to obtain individual ion energies greater than 100 keV , and center of mass energies of several hundred keV with a relatively uncomplicated device. This makes IEC a good technique for studying fusion reactions such as ^3He - ^3He , which until now have only been examined with particle accelerators.³

I.B. The ^3He - ^3He Reaction

The ^3He - ^3He fusion reaction is shown schematically in Fig. 2. The advantages of this reaction over other fusion reactions for electricity generation become obvious when analyzing the reactants and products. The most obvious advantage is that no neutrons are produced. Charged particles are far less likely to induce radioactivity and cause damage than their neutral counterparts. Furthermore, all products generated by this reaction are non-radioactive and non-toxic, making them extremely easy to deal with. These reasons make the ^3He - ^3He fusion cycle very attractive.

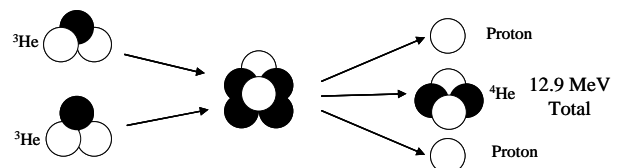


Figure 2: The ^3He - ^3He Reaction

The reactant side of this reaction has advantages and disadvantages. The disadvantages are that ^3He is not readily available at levels for fusion power generation on Earth, and its fusion cross section is very low. However, sources have been found in the near solar system that could be used if there was a market demand.⁴ The advantages are that the reactants are non-radioactive, and non-toxic. Furthermore, since there is only one type of reactant, there are no unwanted reactions that would occur, such as D - D side reactions that would occur in a D - ^3He reactor.

II. THEORY

In traditional IEC systems, gas is flowed into the main vessel, then ionized by Paschen breakdown ($P > 5 \text{ mtorr}$, 0.67 Pa for the UW IEC) or by electrons from hot filaments ($P > 0.2 \text{ mtorr}$, 27 mPa). The positively ionized fuel then gets pulled rapidly to the cathode grid and starts to oscillate through the core. The diagnostics displayed on the left side of Fig. 3 include neutron and proton detectors for measuring fusion reaction products and a residual gas analyzer (RGA) for diagnosing impurity concentrations. An example of a filament assisted discharge IEC device is also shown in Fig. 3:

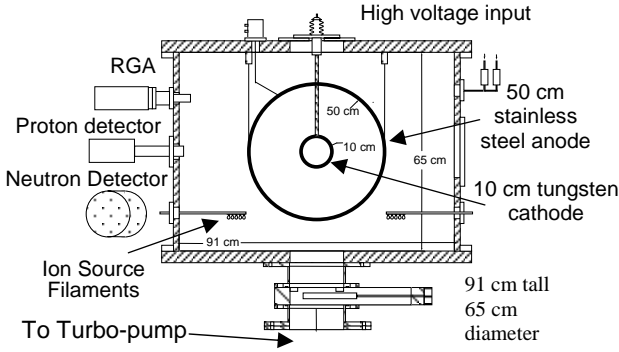


Figure 3: Traditional IEC Device

This configuration is not capable of operating at “low” ($\leq 0.2 \text{ mtorr}$, 27 mPa) pressures, since ionization of the fuel is caused by colliding electrons with it, and at low pressure there are insufficient targets. This limitation leads to a higher pressure operation in which a substantial number of interactions between the recirculating ions and the background gas particles occur. These interactions quickly degrade the ion energy, which prevents many fusion reactions from occurring between ${}^3\text{He}$ atoms. The ${}^3\text{He}$ - ${}^3\text{He}$ reaction cross section is shown in Fig. 4, along with more standard reactions to emphasize the higher energy required.⁵

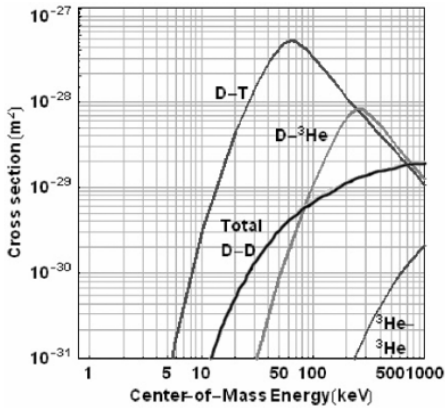


Figure 4: Fusion Cross Sections for Selected Fuels

Since ${}^3\text{He}$ - ${}^3\text{He}$ fusion requires energies at or above 200 keV, an IEC device that operates with little energy loss from collisions with background particles is needed to observe the reactions. If this mode is achieved, the device will operate with recirculating ions that are unattenuated until they intersect the cathode grid. While recirculating, a very small fraction of the ions will collide with the low, though still existent, background gas and fuse. The rate of fusion due to beam-background interactions, df , at any radius r in the device will be proportional to the ion energy E , the background gas density n_b , and the total ion current I_{ion} :

$$df(r) = n_b * \frac{I_{ion}}{e} * \sigma(E) dr \quad (1)$$

where $\sigma(E)$ is the energy dependent fusion cross section, and e is the unit charge. If the system is constructed so that the detection system observes only the reactions inside of the cathode grid, E will be relatively constant as long as there is no substantial charge buildup inside the grid. Furthermore, an expression for I_{ion} that relates to the cathode (measured) current can be written as:

$$I_{ion} = \frac{I_{cath}}{(1 - \eta)(1 + \kappa)} \quad (2)$$

Here I_{cath} is the measured cathode current, η is the cathode transparency, and κ is the average secondary electron emission coefficient of the cathode grid. Furthermore, the assumption is made that the cathode is kept cool enough that there is not a significant emission of thermionic electrons. With a cathode current of 10 mA, and $\eta=0.99$ (99% transparent cathode), and $\kappa = 2$, this gives a total ion current of $\sim 300 \text{ mA}$. Since E does not depend on r inside the cathode, Eq. (1) can be integrated over the cathode diameter to obtain the total fusion rate, F :

$$F = n_b * \frac{I_{cath} * 2R_{cath}}{e(1 - \eta)(1 + \kappa)} * \sigma(E) \quad (3)$$

For the case of $n_b=7*10^{18} \text{ m}^{-3}$ (200 μtorr , 27 mPa), $I_{cath}=10 \text{ mA}$, $R_{cath}=10 \text{ cm}$, $E=200 \text{ keV}$ ($\sigma=8*10^{-32} \text{ m}^2$), and $\eta=0.99$, $\kappa = 2$, F works out to be $\sim 2*10^5 \text{ s}^{-1}$, a measurable number of reactions.⁶

Conversely, this same formula can be used to measure the fusion cross section, as related to a measurement made by a proton detector. The relationship between the count rate the detector observes, D , and the fusion rate F can be expressed as:

$$D = c_{geometry} * c_{efficiency} * F \quad (4)$$

where $c_{geometry}$ and $c_{efficiency}$ are geometric and efficiency calibration factors for the detector being used. For the case of a solid state charged particle detector, the efficiency is effectively 100%, and if the detector is much farther away from the cathode than the cathode radius, the geometry calibration will look like that for a detector observing a point source:

$$D = \frac{F}{4\pi R_{det}^2} A_{det} \quad (5)$$

Where R_{det} is the distance between the detector and the device center, and A_{det} is the detector surface area. Rearranging Eq. (3) and (5) gives an explicit formula for calculating the fusion cross section based on the detector counts observed:

$$\frac{4\pi R_{det}^2 D}{A_{det}} \frac{e(1-\eta)(1+\kappa)}{I_{cath} * 2R_{cath} * n_b} = \sigma(E) \quad (6)$$

III. EXPERIMENTAL SETUP

III.A. IEC Device Setup

For these experiments, it is necessary to avoid any D contamination, since $D-^3\text{He}$ reactions will create a proton signal which might overpower the $^3\text{He}-^3\text{He}$ proton signal, and D gas is known to de-excite helium ions. A new IEC chamber (Fig. 5) and vacuum system was used, that had never been operated with D_2 . The main IEC vacuum chamber consists of a water cooled, stainless steel, spherical shell to allow for long run times if the data collection rate is low. It can be separated in half if necessary, and has six additional ports for diagnostics. For typical operation, a tungsten-rhenium alloy cathode grid is used, due to its combination of high melting point and weldability. The wire which connects the grid to the power supply is surrounded by a 1.9 cm thick boron nitride insulator, a material chosen due to its superior dielectric strength, chemical inertness, and thermal shock resistance. Vacuum is produced by a Varian 450 l/s turbo-molecular pump, which has the capability of pumping the IEC chamber into the ntorr range. The high voltage feedthrough in which the cathode wire connects to the power supply is an oil-filled cylindrical chamber. The high voltage power supply is made by Hipotronics and is capable of steady-state output of 200 kV at up to 75 mA. A port that is sufficiently large to attach the ion sources (to be discussed later) exists at 90 degrees to the axis of the high voltage insulator. The proton detector is a 700 μm thick 1200 mm^2 solid state detector from EG&G-Ortec capable of high resolution charged particle

spectroscopy. This detector will typically be covered with a thin lead foil $\sim 50 \mu\text{m}$ thick to protect the detector from light and minimize x-ray noise.

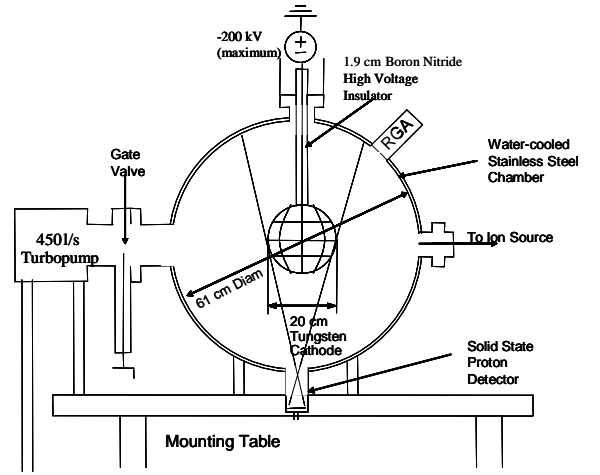


Figure 5: New Water-Cooled IEC device

The proton detector is positioned approximately 50 cm from the device center which gives it a geometrical calibration factor of 2618 fusions/detected count (Eq. (5)). A view of the IEC cathode through a porthole is shown in Fig. 6 during a high pressure glow-discharge mode:

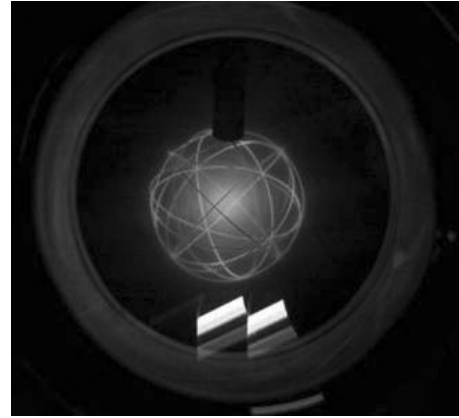


Figure 6: He glow discharge in new IEC chamber with 10 cm diameter cathode (25 kV, 40 mA, 0.67 Pa)

Unlike traditional IEC devices, essentially no ionization takes place inside the main system for these experiments. This is due to the fact that these experiments are operated at low pressure, and significant ionization in the main system will not be possible.

III.B. Helicon Ion Source

In order to provide a source of ions with minimal neutral atom flow, an ion source that takes advantage of the high efficiency ionization associated with helicon

waves has been developed. There are two major parts of the ion source—the helicon plasma generator and the ion extraction region.

The IEC helicon source consists of a 61 cm long, 5 cm diameter quartz tube which is sealed at both ends by silicone o-rings. Vacuum is provided through the ion extraction system and IEC device. Gas is fed in through a mass flow controller. RF power is supplied by a 1400 W ENI 13.56 MHz generator and passed through a shunt/series capacitor matching network. Impedance matching is obtained by adjusting the capacitors, C1 and C2 (in Fig. 7), to minimize reflected power and optimize antenna resonance. The inductive antenna is a Nagoya type III helicon antenna, designed to launch both $m=+1$ and -1 helicon waves. The antenna is made of 0.6 cm copper tubing and requires water cooling to prevent it from melting at high power levels. The axial magnetic field required for helicon discharges is provided by two large water cooled copper electromagnets. Together, these magnets generate 10 gauss/amp, and can run steady state at up to 2 kG. High density ($>10^{18} \text{ m}^{-3}$) helicon discharges can be generated at will in argon and helium. A neutral flow restriction is placed on the front of the quartz tube with a 1 cm^2 discharge hole to reduce neutral flow and limit current to the extraction system. A schematic of the helicon source, and an example of a helicon discharge in argon are shown in Fig. 7 and Fig. 8 respectively.

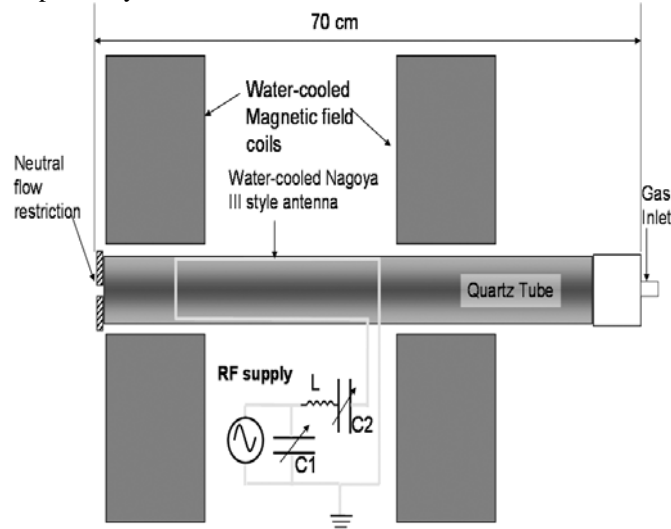


Figure 7: Helicon source schematic

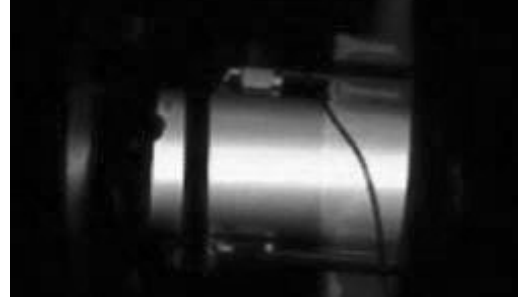


Figure 8: Helicon discharge in argon gas ($B=1\text{kG}$, RF power = 100 W)

A differentially pumped ion extraction region was developed in order to keep neutral pressure low in the IEC device. The system was designed to allow substantial flow of ionized particles while reducing the flow of neutrals. A schematic of the ion source is shown in Fig. 9.

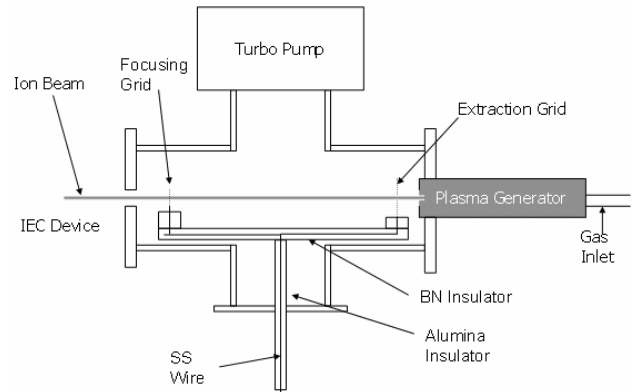


Figure 9: Ion Extraction System

The main vacuum body of the extraction system consists of a 6-way con-flat cross. A port which currently has a window on it is available and would be coming out of the page on the schematic, and a similar port exists on the back for diagnostics. The turbo-pump used for differential pumping is a Varian 250 l/s pump, which can take the extraction system to $< 10 \text{ } \mu\text{torr}$ (1.3 mPa) and probably much lower. The helicon plasma generator connects on the right side by a custom flange modified to accept the o-ring seal discussed above. The extraction and focusing grids are made of tungsten mesh, in order to take the high heat loads from the beam, and are connected to a high voltage wire that brings in power from underneath the vacuum chamber. A Hipotronics 0-30 kV, 0-40 mA power supply is used to supply voltage to the system, and an additional $100 \text{ k}\Omega$ series resistance was added to increase discharge stability. The differential pumping aperture size was chosen to decrease neutral flow by a factor of > 50 . A picture of the helicon,

extraction, and IEC systems joined together is shown in Fig. 10.

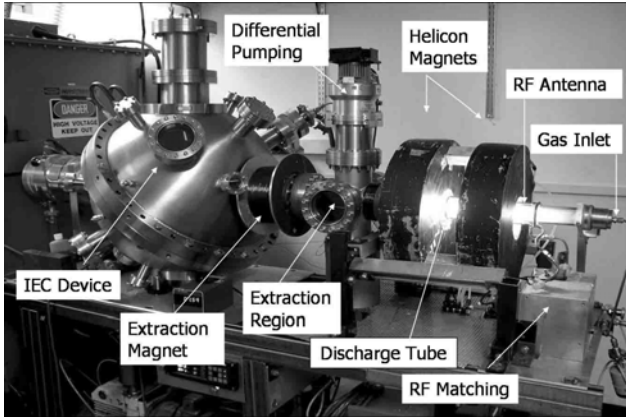


Figure 10: IEC device mated with ion source

IV. RESULTS

Cathode currents in ${}^3\text{He}$ gas have been measured up to 40 mA in the extraction region and near 10 mA in the IEC device. Under these conditions, the background pressure in the device has been kept to 200 μtorr (27 mPa) or less. A picture of a ~ 10 mA ${}^4\text{He}$ ion beam discharging into the device at 30 kV is shown in Fig. 11. Initial experiments with ${}^3\text{He}$ have been conducted up to 140 kV.



Figure 11: He beam discharging into IEC device at $I_{\text{cath}}=10$ mA, $V_{\text{cath}}=30$ kV, 20 mPa

V. CONCLUSIONS

A program to study both low pressure IEC operation and the ${}^3\text{He}$ - ${}^3\text{He}$ fusion reaction is underway at UW-Madison. A new water-cooled IEC vacuum chamber has been constructed and kept free of embedded deuterium to the best extent possible, in order to prevent parasitic D-

${}^3\text{He}$ reactions from overshadowing ${}^3\text{He}$ - ${}^3\text{He}$ reactions. Furthermore, the lack of D gas in the chamber reduces the frequency by which Penning ionization de-excites helium gas, increasing the fraction of ionized helium. Additionally, a high current, low neutral flow ion source has been developed and tested in Ar, ${}^4\text{He}$, and ${}^3\text{He}$ gases. This source allows IEC device operation at pressures low enough so that beam-neutral collisions are insignificant. Such an operating regime allows for good resolution of beam energy and high enough fusion rates for observation. The UW-IEC device can be used to measure ${}^3\text{He}$ - ${}^3\text{He}$ cross sections, as well as demonstrate ${}^3\text{He}$ fusion in an IEC device.

ACKNOWLEDGMENTS

We would like to acknowledge the members of our research group for their thoughtful input on this work. The help of Alex Wehmeyer, Dave Boris, Ross Radel, Tracy Radel, Ben Cipiti, John Weidner, and S. Krupaker Murali was invaluable to the development of this experiment. We would also like to thank Paul Nonn, Greg Winz, and Noah Hershkowitz for their time and their tremendous expertise in the various topics needed to make this all happen. Finally, we would like to thank the Grainger Foundation, the Greatbatch Foundation, and the University of Wisconsin for providing material support, without which none of this would be possible.

REFERENCES

- [1] PHILO T. FARNSWORTH, "Electric Discharge Device for Producing Interactions between Nuclei," United States Patent Office #3,258,402, June 28, (1966).
- [2] R. L. HIRSCH, "Inertial-Electrostatic Confinement of Ionized Fusion Gasses," J. Apl. Phys. **38**, 4522 (1967).
- [3] M. R. Dwarakanath, et al, " ${}^3\text{He}({}^3\text{He},2p){}^4\text{He}$ Total Cross Section Measurements Below the Coulomb Barrier," Physical Review C, **4**, 5 1532 (1971).
- [4] L. J. WITTENBERG, J. F. SANTARIUS, AND G. L. KULCINSKI, "Lunar Source of ${}^3\text{He}$ for Commercial Fusion Power," Fusion Technology **10**, 167 (1986).
- [5] RAINER FELDBACHER, *Nuclear Reaction Cross Sections and Reactivity Parameter Library and Files--The AEP Barnbook DATLIB*, International Nuclear Data Committee, (1987).
- [6] R.P. ASHLEY, G.L. KULCINSKI, J.F. SANTARIUS, S. KRUPAKAR MURALI, G. PIEFER, *D- ${}^3\text{He}$ Fusion in an Inertial Electrostatic Confinement Device*, 18th Symposium on Fusion Engineering, IEEE Publication 99CH37050, 35, October (1999).